Equivalent Circuit Modeling of Piezoelectric Energy Harvesters

YAOWEN YANG* AND LIHUA TANG

School of Civil and Environmental Engineering, Nanyang Technological University, 50 Nanyang Avenue, 639798 Singapore

ABSTRACT: Last decade has seen growing research interest in vibration energy harvesting using piezoelectric materials. When developing piezoelectric energy harvesting systems, it is advantageous to establish certain analytical or numerical model to predict the system performance. In the last few years, researchers from mechanical engineering established distributed models for energy harvester but simplified the energy harvesting circuit in the analytical derivation. While, researchers from electrical engineering concerned the modeling of practical energy harvesting circuit but tended to simplify the structural and mechanical conditions. The challenges for accurate modeling of such electromechanical coupling systems remain when complicated mechanical conditions and practical energy harvesting circuit are considered in system design. In this article, the aforementioned problem is addressed by employing an equivalent circuit model, which bridges structural modeling and electrical simulation. First, the parameters in the equivalent circuit model are identified from theoretical analysis and finite element analysis for simple and complex structures, respectively. Subsequently, the equivalent circuit model considering multiple modes of the system is established and simulated in the SPICE software. Two validation examples are given to verify the accuracy of the proposed method, and one further example illustrates its capability of dealing with complicated structures and non-linear circuits.

Key Words: energy harvesting, piezoelectric materials, finite element analysis, equivalent circuit model.

INTRODUCTION

CURRENT wireless sensing applications or portable electronics are designed to include external power supply, which requires periodical maintenance for long-term operation. With advancement of low-power electronics, continuously self-powered wireless sensing systems are coming from concept to practice. As one ubiquitous energy form in our daily life, vibration is a promising ambient source for energy harvesting. There exist several basic mechanisms for vibration-to-electrical energy conversion. Using piezoelectric material is one of the most popular ways, attractive for its high energy density. In the past few years, significant research efforts have been devoted to vibration energy harvesting using piezoelectric materials (Anton and Sodano, 2007).

During the design stage of a piezoelectric energy harvester, it is important to establish certain analytical or numerical model to estimate the output power of the system. Some analytical models are already available in the literature. Erturk and Inman (2008a) established an analytical distributed parameter model for cantilevered piezoelectric energy harvesters. Liao and Sodano (2008) developed a theoretical model of piezoelectric energy harvesting system to predict the power around a single vibration mode based on the Rayleigh–Ritz approach. However, these researches focused on the maximum power that can be achieved by simplifying the energy harvesting circuit as a resistor or some combination of linear electrical elements (Liao and Sodano, 2009). In reality, the circuit attached to an energy harvester is more complicated than a resistor for current regulation and power management. Theoretical analysis is very difficult when some non-linear electrical components are included. On the other hand, some researchers, usually from electrical engineering, focused on developing models with non-linear circuit techniques, such as synchronized switch harvesting on inductor technique (Badel et al., 2005; Lefeuvre et al., 2005), and simplified the structure as a single degree of freedom system. However, these models cannot account for higher vibration modes of the energy harvester. It is obvious that all the models aforementioned can only be applied for evaluation of system performance in some specific conditions, where either the mechanical or electrical condition is much simplified. The challenge remains to establish a more general modeling approach to account for both complex mechanical conditions and practical energy harvesting circuit.

Finite element analysis (FEA) and SPICE software are powerful tools in structural and electrical engineering,

respectively. Using FEA, it is easy to estimate the open-circuit voltage or short-circuit current of the piezoelectric energy harvester. Unfortunately, the calculated results cannot be applied in the SPICE simulation to evaluate the system performance unless the electromechanical coupling is weak and negligible. When the electromechanical coupling is strong, the backward coupling force will affect the mechanical vibration and hence the voltage or current source is not constant with various electric loads. Elvin and Elvin (2009a) proposed one general equivalent circuit model for piezoelectric energy harvesters, which considered the backward coupling effect in the mechanical domain and multiple vibration modes. The parameters of equivalent circuit were derived using the Rayleigh–Ritz approach. However, this approach required accurate assumption of mode shapes and usually considered a large number of assumed modes, which were challenging for complicated structures. To avoid this difficulty and utilize the available powerful tools in structural and electrical modeling, Elvin and Elvin (2009b) developed a coupled FEA–SPICE simulation model for analyzing piezoelectric energy generators. However, in this model, an automation program is needed to extract nodal displacements from the FEA output and coupling voltage from the SPICE output, and then transfer these data between the FEA and SPICE solvers at each iteration. However, a new difficulty accompanied is that for a complicated model, the post-process of data extraction and transfer is quite difficult to implement and tedious even for one iteration, which limits the applicability of this simulation model. The challenge now is to enable efficient collaboration of robust FEA and SPICE solvers and exert their respective advantages, and meanwhile take into account the backward coupling effect.

In this article, an efficient method based on the equivalent circuit model (ECM) is developed to bridge the FEA and SPICE simulation for accurate estimation of performance of piezoelectric energy harvesters. According to different mechanical conditions, the system parameters used in the equivalent circuit model are determined by theoretical analysis or FEA. Numerical examples are presented to validate the accuracy of the developed equivalent circuit model and to illustrate its capability of dealing with complicated structures and non-linear circuits. Finally, together with the proposed ECM-based modeling method, other modeling techniques for piezoelectric energy harvesters and their applicability are summarized.

ANALYTICAL MODELING

A reliable analytical model provides useful insight into characteristics of piezoelectric energy harvesting system. Several mathematical models have been established in the past few years, including uncoupled and coupled single degree of freedom (SDOF) models,

uncoupled and coupled distributed parameter models as well as approximate distributed parameter models derived by the Rayleigh–Ritz approach. Erturk and Inman (2008b) reviewed these models and clarified some misleading modeling issues on piezoelectric energy harvesting. Here we give a brief introduction of the distributed parameter model for a simple cantilevered unimorph harvester, established by Erturk and Inman (2008a). The energy harvester with bimorph configuration can be derived similarly.

The unimorph cantilever beam is shown in Figure 1. The profile of energy harvester is rectangular and the density of beam along the longitudinal direction is uniform. The analytical model is derived based on the constitutive relations of piezoelectricity and the following assumptions: (a) Euler–Bernouli beam assumption; (b) negligible external excitation from air damping; (c) proportional damping (i.e., the strain rate damping and viscous air damping are assumed to be proportional to the bending stiffness and mass per length of the beam); and (d) uniform electric field through the piezoelectric thickness.

The e-form piezoelectric constitutive relations are:

$$
\begin{aligned}
T_1 &= Y_1^E S_1 - e_{31} E_3, \\
D_3 &= e_{31} S_1 + \varepsilon_{33}^S E_3,
\end{aligned}
\tag{1}
$$

where T_1 and S_1 are the stress and strain components in the piezoelectric layer along 1-direction (longitudinal direction), respectively; D_3 and E_3 are the electric displacement and electric field along 3-direction (thickness direction), respectively; Y_1^E and ε_{33}^S are the Young's modulus and electric permittivity of the piezoelectric layer, respectively; the superscripts E and S indicate that the parameters are measured at constant electric field (short-circuit) and at constant strain (beam is totally clamped), respectively; and e_{31} is the piezoelectric constant. Based on assumptions (a) and (b), the governing equation of mechanical motion is:

$$
\frac{\partial^2 M(x,t)}{\partial x^2} + c_s I \frac{\partial^5 w_{\text{rel}}(x,t)}{\partial x^4 \partial t} + c_a \frac{\partial w_{\text{rel}}(x,t)}{\partial t} + m \frac{\partial^2 w_{\text{rel}}(x,t)}{\partial t^2}
$$
$$
= -m \frac{\partial^2 w_b(x,t)}{\partial t^2},
\tag{2}
$$
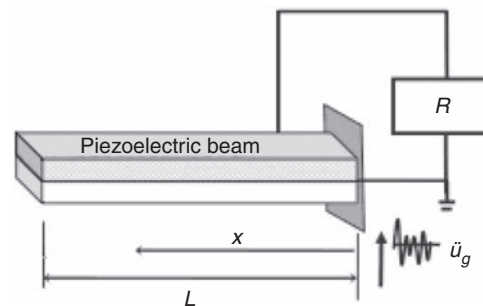
Figure 1. Rectangular unimorph energy harvester subjected to base excitation.

where $M(x,t)$ is the internal bending moment of the beam; I is the equivalent area moment of inertia of the composite cross section; $w_b(x,t)$ and $w_{\mathrm{rel}}(x,t)$ are the base excitation and the deflection relative to the base motion, respectively; c_s and c_a are the strain rate damping coefficient and viscous air damping coefficient, respectively; m is the mass per unit length; x is the longitudinal coordinate and t is time. Applying the first constitutive equation and expressing the moment by integrating stress distribution over the composite cross section of the beam, and considering assumption (d), we obtain:

$$YI\frac{\partial^4 w_{\mathrm{rel}}(x,t)}{\partial x^4} + c_s I\frac{\partial^5 w_{\mathrm{rel}}(x,t)}{\partial x^4 \partial t} + c_a\frac{\partial w_{\mathrm{rel}}(x,t)}{\partial t} + m\frac{\partial^2 w_{\mathrm{rel}}(x,t)}{\partial t^2}$$
$$+ \theta V(t)\left[\frac{\mathrm{d}\delta(x)}{\mathrm{d}x} - \frac{\mathrm{d}\delta(x-L)}{\mathrm{d}x}\right] = -m\frac{\partial^2 w_b(x,t)}{\partial t^2}, \quad (3)$$

where YI is the average bending stiffness; θ is the electromechanical coupling coefficient; $V(t)$ is the output voltage of the energy harvester; and $\delta(x)$ is the Dirac delta function. Integrating the second constitutive equation over the area of piezoelectric layer and differentiating it with respect to t, we obtain:

$$\frac{V(t)}{R_l} + C^S\frac{\mathrm{d}V(t)}{\mathrm{d}t} + \int_0^L e_{31}h_{pc}b\frac{\partial^3 w_{\mathrm{rel}}(x,t)}{\partial x^2 \partial t}\mathrm{d}x = 0, \quad (4)$$

where C^S is the capacitance measured at constant strain, corresponding to the clamped electric permittivity ε_{33}^S; R_l is the resistance of the attached resistive load; b is the width of the beam; h_{pc} is the distance from the center of the piezoelectric layer to neutral axis of the beam. Based on assumption (c), the vibration response relative to the base can be represented as an absolute and uniform convergent series of the eigenfunctions as:

$$w_{\mathrm{rel}}(x,t) = \sum_{r=1}^{\infty} \phi_r(x)\eta_r(t), \quad (5)$$

where $\varphi_r(x)$ and $\eta_r(t)$ are the mass normalized eigenfunctions and the modal coordinate of the r-th mode, respectively. Substituting Equation (5) into Equations (3) and (4), the electromechanical coupled ordinary differential equations for the modal response of the beam can be obtained as:

$$\frac{\mathrm{d}^2\eta_r(t)}{\mathrm{d}t^2} + 2\zeta_r\omega_r\frac{\mathrm{d}\eta_r(t)}{\mathrm{d}t} + \omega_r^2\eta_r(t) + \chi_r V(t) = -f_r\ddot{u}_g(t), \quad (6)$$

$$\frac{V(t)}{R_l} + C^S\frac{\mathrm{d}V(t)}{\mathrm{d}t} - \sum_{r=1}^{\infty}\chi_r\frac{\mathrm{d}\eta_r(t)}{\mathrm{d}t} = 0, \quad (7)$$

where ω_r and ζ_r are the natural frequency and damping ratio of the r-th mode; χ_r is the modal electromechanical coupling coefficient; and $-f_r\ddot{u}_g(t)$ is the modal mechanical forcing function.

$$\chi_r = \int_0^L \theta\left[\frac{\mathrm{d}\delta(x)}{\mathrm{d}x} - \frac{\mathrm{d}\delta(x-L)}{\mathrm{d}x}\right]\phi_r(x)\mathrm{d}x$$
$$= \int_0^L \theta\frac{\mathrm{d}^2\phi_r(x)}{\mathrm{d}x^2}\mathrm{d}x = \theta\frac{\mathrm{d}\phi_r(x)}{\mathrm{d}x}\Big|_{x=L}, \quad (8)$$

$$f_r = \int_0^L m\phi_r(x)\,\mathrm{d}x. \quad (9)$$

When the harmonic base excitation $u_g(t) = Ae^{j\omega t}$ is applied (j is the unit imaginary number and ω is the excitation frequency), the steady state voltage response across the resistive load can be expressed as:

$$V(t) = i(t)\cdot R_l$$
$$= \frac{\displaystyle\sum_{r=1}^{\infty} j\omega\chi_r f_r/(\omega_r^2 - \omega^2 + j2\zeta_r\omega_r\omega)}{\displaystyle\sum_{r=1}^{\infty} j\omega\chi_r^2/(\omega_r^2 - \omega^2 + j2\zeta_r\omega_r\omega) + j\omega C^S + \frac{1}{R_l}} A\omega^2 e^{j\omega t}, \quad (10)$$

where $i(t)$ is the current through the resistive load.

SYSTEM-LEVEL FINITE ELEMENT MODELING

To achieve optimal system performance, multilayer piezoelectric energy harvesters are usually used, and the profile of energy harvester is not necessarily designed as shown in Figure 1. Roundy et al. (2005) pointed out that with the same volume of PZT, some alternative mechanical structures can significantly increase energy harvesting performance. For example, a trapezoidal cantilever beam, which distributes the strain more evenly such that maximum strain is attained at each point on the surface of the beam, can supply more than twice the amount of energy than a rectangular beam. In such case, the parameters of beam, i.e., YI, m, θ, h_{pc} and b in Equations (3) and (4) should be replaced by $YI(x)$, $m(x)$, $\theta(x)$, $h_{pc}(x)$, and $b(x)$, respectively. Hence, χ_r and f_r should be written as:

$$\chi_r = \int_0^L \theta(x)\frac{\mathrm{d}^2\phi_r(x)}{\mathrm{d}x^2}\mathrm{d}x, \quad (11)$$

$$f_r = \int_0^L m(x)\phi_r(x)\,\mathrm{d}x. \quad (12)$$

However, in such case, theoretical derivation of mode shape functions and parameters χ_r and f_r at each resonance is a tough task. To avoid this difficulty, FEA can be used to estimate the response of the piezoelectric energy harvester. Several robust commercial codes such as ABAQUS and ANSYS allow for the modeling of piezoelectric transducer as both actuator and generator (energy harvester). Although various circuit elements from resistors to diodes are available in the element library of ANSYS, only the basic linear circuit elements such as capacitor, inductor and resistor are compatible with the piezoelectric elements. This limits the applicability of system-level FEA. However, if one's concern is to estimate the maximum achievable power from the energy harvester, linear circuit elements are adequate for system-level simulation in ANSYS.

A finite element model for system-level simulation is shown in Figure 2. In this model, the voltage degrees of freedom on the top and bottom surfaces of the piezoelectric layer are coupled separately to implement uniform electrical potentials on the top and bottom electrodes. It is to be noted that Figure 2 is just an illustration on how to model a piezoelectric energy harvester

in ANSYS. In the later part of this article, the mesh of the finite element model is further refined.

EQUIVALENT CIRCUIT MODELING

Generally, the analytical models and system-level FEA are only applicable to estimate the maximum power available to be extracted from a piezoelectric energy harvester by connecting a resistive load. In practice, however, an energy harvesting circuit is required to include some non-linear electric components such as rectifier and regulator as well as an energy storage module. A practical energy harvesting circuit may look like the one shown in Figure 3. Furthermore, if the geometry of energy harvester is complicated so as to achieve optimal system performance (as mentioned in the previous section), modeling of the energy harvesting system will be more challenging. Neither the analytical models nor the system-level FEA is able to address these issues. An equivalent circuit modeling method is thus proposed in this work to solve these problems. However, different from the approach of Elvin and Elvin (2009a), the parameters of equivalent circuit in the current method can be conveniently extracted from FEA results for
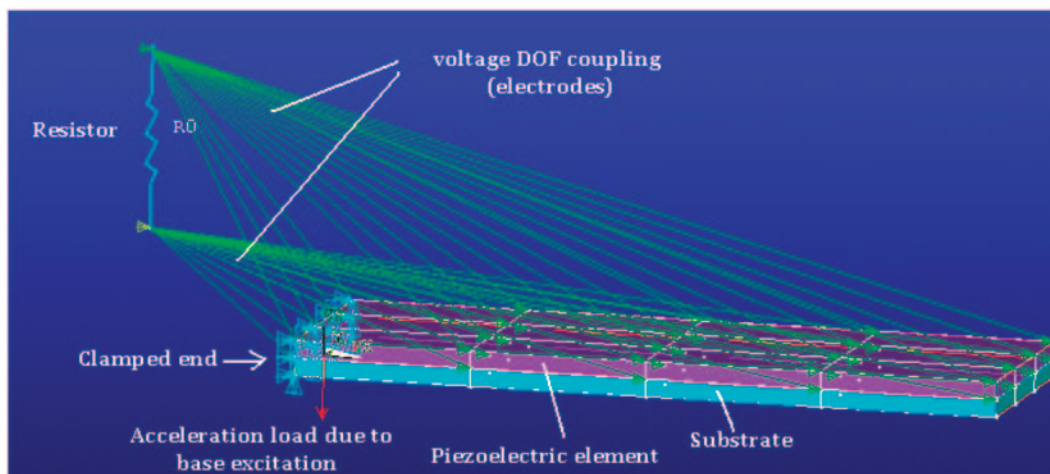

Figure 2. Finite element model for system-level simulation.
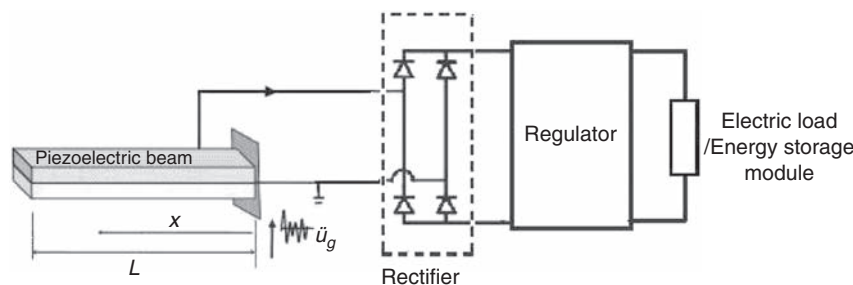

Figure 3. Practical energy harvesting circuit.

Table 1. Analogy between electrical and mechanical domains.

Equivalent circuit parameters at r-th mode	Mechanical counterparts
Charge: $q_r(t)$	Modal coordinate: $\eta_r(t)$
Current: $i_r(t)$	Modal velocity: $d\eta_r(t)/dt$
Inductance: L_r	1
Resistance: R_r	$2\zeta_r\omega_r$
Capacitance: C_r	$1/\omega_r^2$
Voltage source: $V_r(t)$	$-f_r\ddot{u}_g(t)$
Ideal transformer ratio: N_r	Electromechanical coupling: χ_r

complicated structures, avoiding the tedious calculation by the Rayleigh–Ritz approach.

In Equations (6) and (7), it is observed that an analogy exists between the mechanical and electrical domains of the piezoelectric coupling system, as illustrated in Table 1. Actually, the equivalent circuit representations of electromechanical transducers have been studied for a long time. Tilmans (1996, 1997) have summarized the equivalent circuit models for various electromechanical transducers, including the piezoelectric transducer. In this article, a method based on equivalent circuit model is developed to address the challenges of traditional approaches. Once the equivalent circuit parameters are determined, the performance of energy harvesting system can be evaluated by the SPICE simulation. The remaining issue is thus identification of the required parameters.

Here, we consider two cases, i.e., a simple and a complex mechanical condition of the energy harvester. The simple mechanical condition refers to simple geometric configuration and simple mechanical boundaries. The complex mechanical condition refers to non-uniform beam configuration and complex mechanical boundaries. For the first case, the parameters in the equivalent circuit model can be directly obtained by analogizing Equations (6) and (7) with circuitry differential equations. For the second case, a parameter identification method by FEA will be proposed. It should be mentioned that no matter in which case, the basis for parameter identification is the analogy between the electrical and mechanical domains. Since the mechanical motion Equation (3) implies the small deformation of energy harvester, non-linear structural behavior cannot be taken into account by the proposed equivalent circuit modeling method.

Equivalent Circuit Model with Theoretically Derived Parameters

After theoretical modal analysis, we can determine the corresponding parameters C_r, L_r, R_r, N_r, and $V_r(t)$

which will be used in the equivalent circuit model, as listed in Table 1, by analogizing Equations (6) and (7) with the differential equations of a circuit network. The circuit network consists of infinite branches, each composed of an inductor, a capacitor, a resistor, an ideal voltage source and an ideal transformer, as shown in Figure 4. The r-th circuit branch represents the r-th vibration mode of the system. It is noted that Equations (6) and (7) satisfy Kirchoff's voltage and current laws respectively, after equivalent circuit representation. In Equations (8) and (9), the integrals may give positive or negative values. Since the SPICE software only accepts positive input value, we can change the wire connection pattern when the ideal voltage magnitude or transformer ratio is negative from the integrals (8) and (9). For example, if the transformer ratio N_2 is negative in Figure 4, the terminals of capacitor C^S and transformer should be connected with the pattern: '+'→'−', '−' →'+'.

The procedure to evaluate the system performance includes the following steps:

(A) Theoretical modal analysis to obtain the natural frequencies and mode shape functions of the energy harvester;
(B) Determining the equivalent circuit parameters through analogies; and
(C) System modeling in the SPICE software with the determined parameters.

Equivalent Circuit Model with Parameters Identified by FEA

As mentioned in the previous section to achieve optimal system performance, the geometry of the energy harvester could be more complicated and the harvester may have complex mechanical boundaries. In such case, it is difficult to theoretically derive the parameters of equivalent circuit model. Here we propose a parameter identification method based on FEA. The parameters to be identified are C_r, L_r, R_r, N_r, and $V_r(t)$. The first four parameters will be identified from the admittance of piezoelectric energy harvester, and subsequently, the last parameter $V_r(t)$ will be determined from the short-circuit charge response with base excitation.

IDENTIFICATION OF C_r, L_r, R_r, *AND* N_r
To obtain the admittance of piezoelectric transducer, a harmonic voltage $V(t)$ is applied to the energy harvester. Hence, replacing $V(t)/R_l$ with $-i(t)$ in Equation (7), setting $-f_r\ddot{u}_g(t)$ to zero in Equation (6) and transforming the two equations into frequency domain,
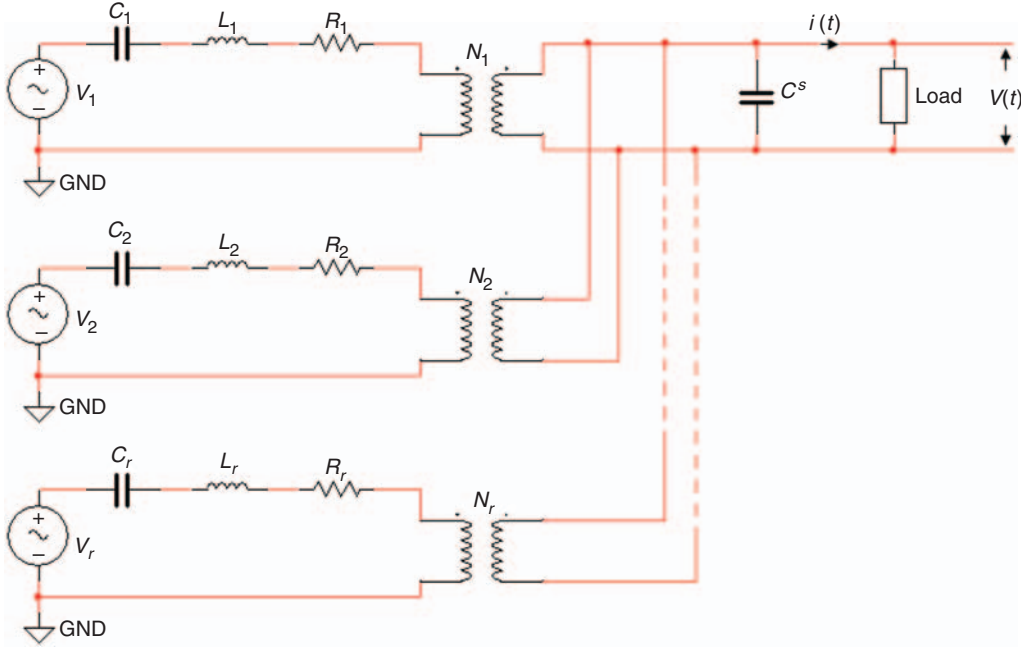
Figure 4. Multi-mode equivalent circuit model.

we can obtain the admittance Y as:

$$Y = \frac{i}{V} = \frac{j\omega Q}{V} = j\omega \left(C^S + \sum_{r=1}^{\infty} \frac{\chi_r^2}{\omega_r^2 - \omega^2 + j2\zeta_r\omega_r\omega} \right). \quad (13)$$

Here, the negative sign of $-i(t)$ means that the current flows into the system, as shown in Figure 5, since now the piezoelectric transducer works as an actuator. This is different from the current flow direction in Figure 4, in which the transducer works as a generator (energy harvester). Applying the analogies list in Table 1 to Equation (13), we obtain:

$$Y = j\omega \left(C^S + \sum_{r=1}^{\infty} \frac{N_r^2}{\frac{1}{C_r} - L_r\omega^2 + jR_r\omega} \right). \quad (14)$$

According to the properties of an ideal transformer, the impedance in the circuit is transformed by the square of turn ratio. Hence, L_r, R_r, and C_r can be converted from the left side of the transformer to the right side using the following relations, as shown in Figure 5.

$$L_{mr} = \frac{L_r}{N_r^2}, \quad R_{mr} = \frac{R_r}{N_r^2}, \quad C_{mr} = C_r N_r^2 \quad (15)$$

Rearranging Equation (14), we obtain:

$$Y = j\omega \left(C^S + \sum_{r=1}^{\infty} \frac{C_{mr}}{1 - L_{mr}C_{mr}\omega^2 + jR_{mr}C_{mr}\omega} \right). \quad (16)$$

The resonance frequency and quality factor (Ikeda, 1990) can be written as:

$$\omega_r = \frac{1}{\sqrt{L_{mr}C_{mr}}}, \quad Q_{mr} = \frac{\omega_r}{\omega_1 - \omega_2} = \frac{1}{R_{mr}}\sqrt{\frac{L_{mr}}{C_{mr}}}$$

$$= \frac{1}{R_{mr}C_{mr}\omega_r} = \frac{\omega_r L_{mr}}{R_{mr}}, \quad (17)$$

where ω_1 and ω_2 are the half-width frequencies near the r-th resonance.

Consider the following three cases:

(1) $\omega \to 0$, from Equation (16), we obtain:

$$Y \to j\omega \left(C^S + \sum_{r=1}^{\infty} C_{mr} \right) = j\omega C^T, \quad (18)$$

where C^T is the static capacitance measured when no external mechanical force is applied on the energy harvester.

(2) $\omega \to \infty$, from Equation (16), we obtain:

$$Y \to j\omega C^S, \quad (19)$$

where C^S is the static clamped capacitance. The result is understandable because when the frequency of applied voltage approaches infinity, the structure deformation cannot accompany with the alternating electric field. Hence the boundary condition is similar to the case that the harvester is totally clamped.
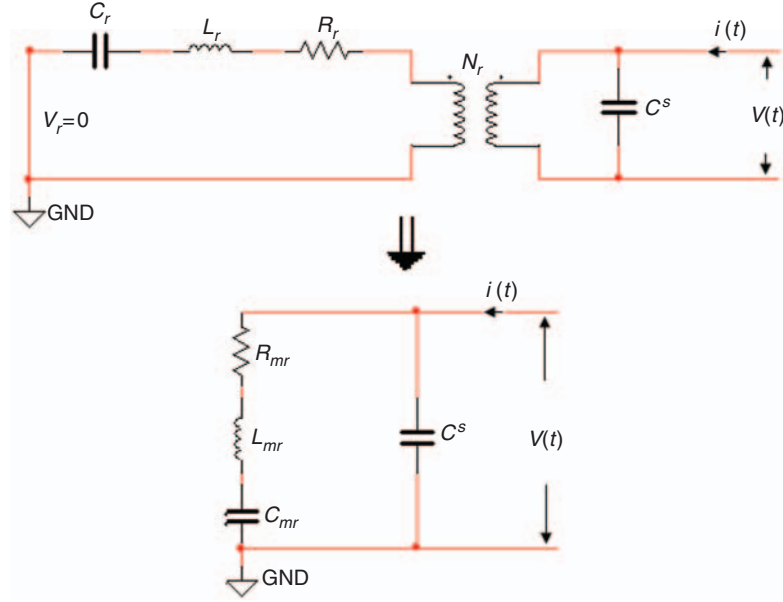
Figure 5. The r-th branch of equivalent circuit model of piezoelectric transducer in actuator mode.

(3) $\omega \rightarrow \omega_r$, we can derive the admittance as follows:

$$Y = j\omega \left(\begin{array}{c} C^S + \dfrac{C_{m1}}{1 - L_{m1}C_{m1}\omega^2 + jR_{m1}C_{m1}\omega} \\ + \dfrac{C_{m2}}{1 - L_{m2}C_{m2}\omega^2 + jR_{m2}C_{m2}\omega} + \\ \cdots + \dfrac{C_{mr}}{1 - L_{mr}C_{mr}\omega^2 + jR_{mr}C_{mr}\omega} + \cdots \end{array} \right)$$

$$\approx j\omega \left(C^S + \underbrace{0 \cdots 0}_{r-1} + \frac{C_{mr}}{1 - L_{mr}C_{mr}\omega^2 + jR_{mr}C_{mr}\omega} + \sum_{i=r+1}^{\infty} C_{mi} \right)$$

$$= j\omega \left(C^T - \sum_{i=1}^{r} C_{mi} + \frac{C_{mr}}{1 - L_{mr}C_{mr}\omega^2 + jR_{mr}C_{mr}\omega} \right)$$

$$= j\omega \left(C_{dr} + \frac{C_{mr}}{1 - L_{mr}C_{mr}\omega^2 + jR_{mr}C_{mr}\omega} \right)$$

$$= Y_d + Y_{\mathrm{mot}}, \tag{20}$$

where Y_d and Y_{mot} are termed damped admittance and motional admittance (Ikeda, 1990), respectively.

$$Y_d = j\omega C_{dr} \tag{21}$$

$$Y_{\mathrm{mot}} = \frac{j\omega C_{mr}}{1 - L_{mr}C_{mr}\omega^2 + jR_{mr}C_{mr}\omega} \tag{22}$$

The approximation in Equation (20) can be understood by substituting Equation (17) into it and examining the denominators term by term. The locus of Y_{mot} in the complex plane near the r-th resonance is an approximate circle whose equation can be written as:

$$\left[\mathrm{Re}(Y_{\mathrm{mot}}) - \frac{1}{2R_{mr}} \right]^2 + [\mathrm{Im}(Y_{\mathrm{mot}})]^2 = \left(\frac{1}{2R_{mr}} \right)^2. \tag{23}$$

C_{dr} is termed damped capacitance (Ikeda, 1990) at the r-th vibration mode. It should be noted that C_{dr} is not equal to C^S as it also includes the contribution from the higher modes ($r + 1$ and above). Hence, when we draw the approximate circle of Y_{mot} of each mode, different Y_d should be excluded from the total admittance Y, according to different C_{dr}:

$$C_{dr} = C^T - \sum_{i=1}^{r} C_{mi}. \tag{24}$$

From Equation (20), we know that C_{dr} can be directly extracted from FEA results according to:

$$C_{dr} = \mathrm{Im}[Y(\omega_r)]. \tag{25}$$

Then draw the admittance locus of Y_{mot} of each vibration mode, which is an approximate circle as described by Equation (23), and consider Equation (17), we can identify parameters C_{mr}, L_{mr}, R_{mr}, and N_r as:

$$\begin{cases} R_{mr} = \dfrac{1}{2 \cdot \mathrm{raduis}} = \dfrac{1}{\max[\mathrm{Re}(Y_{\mathrm{mot}})]} \\[2mm] L_{mr} = \dfrac{R_{mr}}{\omega[\min[\mathrm{Im}(Y_{\mathrm{mot}})]] - \omega[\max[\mathrm{Im}(Y_{\mathrm{mot}})]]} \\[2mm] C_{mr} = \dfrac{1}{\omega_r^2 L_{mr}} \\[2mm] N_r = \sqrt{\dfrac{1}{L_{mr}}} \end{cases} \tag{26}$$

Parameter N_r is obtained in the above equation. According to Equation (15), we can determine the other three parameters C_r, L_r, and R_r. Here, we have no concern for the sign of N_r, which will be clarified in the following section.

IDENTIFICATION OF $V_r(t)$

The last undetermined parameter in the equivalent circuit model is $V_r(t)$. If a unit harmonic base acceleration is applied to the system, the magnitude of $V_r(t)$ is f_r. Given short-circuit condition, according to Equation (10), we can obtain from FEA the charge response at each resonance frequency ω_r as:

$$
\begin{aligned}
Q(j\omega_r) &= \chi_r \eta_r(j\omega_r) \\
&= \frac{\chi_r f_r}{\omega_r^2 - \omega^2 + j2\zeta_r\omega_r\omega}\bigg|_{\omega=\omega_r} \\
&= \frac{\chi_r f_r}{\chi_r^2 R_{mr} j\omega_r} = \frac{f_r}{N_r R_{mr} j\omega_r}.
\end{aligned} \tag{27}
$$

Hence, with the obtained N_r and R_r, we can calculate f_r as:

$$
f_r = N_r R_{mr} j\omega_r Q(j\omega_r). \tag{28}
$$

The sign of $\chi_r f_r$ can be determined according to the phase angle of the charge response by FEA. Furthermore, in Equation (10), it should be noted that it is the sign of $\chi_r f_r$ that affects the response of the system rather than the sign of χ_r or f_r alone. Hence, we need not determine the sign of χ_r or f_r alone. Actually, from the viewpoint of circuit, there is no change in the flow direction of the output current if we change at the same time the terminal wiring pattern of the ideal transformer and the ideal voltage source of one circuit branch in Figure 4.

GENERAL PROCEDURE OF EQUIVALENT CIRCUIT MODELING

In summary, the general procedure of equivalent circuit modeling to evaluate the performance of the energy harvester is as follows:

(A) Finite element static analysis to determine the static capacitance C^T and C^S;
(B) Finite element modal analysis to determine the short-circuit resonance frequency of each vibration mode;
(C) Finite element harmonic analysis to obtain the charge response and then the admittance with a harmonic alternating voltage input. Identify the parameters C_r, L_r, R_r, and N_r from each admittance circle of Y_{mot};
(D) Finite element harmonic analysis to obtain the charge response at each resonance, with base excitation applied, to determine $V_r(t)$;

(E) Circuit modeling and simulation in the SPICE software with the parameters identified from FEA to evaluate the performance of energy harvester.

MODEL VALIDATION

Two examples are investigated in this section to validate the equivalent circuit modeling method presented in the section 'Equivalent Circuit Modeling'. For Examples 1 and 2, the parameters used in the equivalent circuit models are identified by theoretical analysis and FEA, respectively. A further example is also presented to show the capability and applicability of the proposed ECM-based method for the case in which complicated mechanical condition and practical energy harvesting circuit are considered.

Validation Example 1

The first validation example considers a simple rectangular piezoelectric beam with unimorph configuration. A resistor is attached to the beam to represent the energy harvesting circuit, as shown in Figure 1. Since the geometry of the energy harvester is simple, the parameters of the equivalent circuit model are derived by theoretical analysis, as depicted in the section 'Equivalent Circuit Model with Theoretically Derived Parameters'. Although the equivalent circuit model can account for more complicated practical energy harvesting circuit, only a resistor is considered here so that the results can be compared with those obtained by the analytical model and system-level FEA. All geometric and material properties of the energy harvester are listed in Table 2.

We consider the first three vibration modes of the system in the frequency range of 0–1000 Hz. A multi-mode equivalent circuit model is established with the

Table 2. Properties of uniform beam with unimorph piezoelectric layer.

Item	Value
Young's modulus of piezoelectric layer	66 GPa
Young's modulus of substrate layer	100 GPa
Density of piezoelectric layer	7800 kg/m³
Density of substrate layer	7165 kg/m³
Clamped permittivity of piezoelectric layer ε_{33}^S	1.593e−8 F/m
Piezoelectric constant e_{31}	−12.54 C/m²
Rayleigh damping constant a	4.894
Rayleigh damping constant β	1.2349e−5
Beam length L	100 mm
Beam width b	20 mm
Thickness of piezoelectric layer h_p	0.4 mm
Thickness of substrate layer h_s	0.5 mm

parameters determined from theoretical analysis as listed in Table 3. Figures 6–8 compare the magnitude and phase of the output voltage and power of the energy harvesting system from the equivalent circuit model, analytical model and system-level FEA for five different resistive loads. It is observed that the results of equivalent circuit model match perfectly with those from the analytical model and system-level FEA. In Figure 8, it should be noted that the maximum power is obtained at different frequency with different electric loads, which is caused by the backward electromechanical coupling effect on vibration. Hence, it validates that the equivalent circuit modeling is capable of accounting for this backward coupling effect as the system-level FEA and analytical model (Erturk and Inman, 2008a) do.

Validation Example 2

The second validation example considers an isosceles trapezoidal piezoelectric beam with unimorph configuration, as shown in Figure 9(a). Again, a single resistor of $1\,M\Omega$ is attached for the convenience of comparing the equivalent circuit model with the system-level FEA.

Table 3. Parameters of equivalent circuit model determined from theoretical analysis.

| *r*-th mode	N_r	L_r	R_r	C_r	f_r
1	0.017563	1	6.00833	1.1082E−05	0.090655
2	−0.06010	1	48.6582	2.82171E−07	0.050241
3	0.10014	1	348.013	3.59905E−08	0.029457
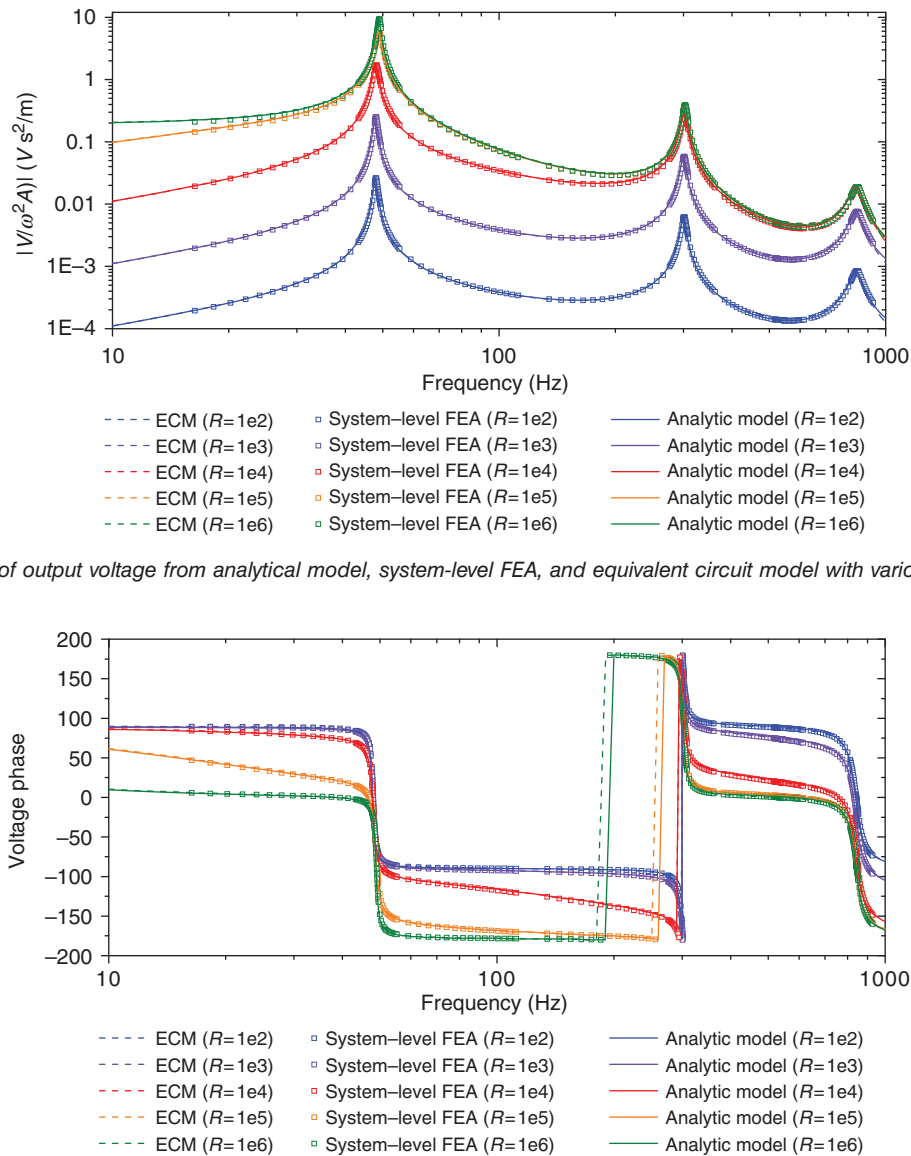
Figure 6. *Magnitude of output voltage from analytical model, system-level FEA, and equivalent circuit model with various resistive loads.*
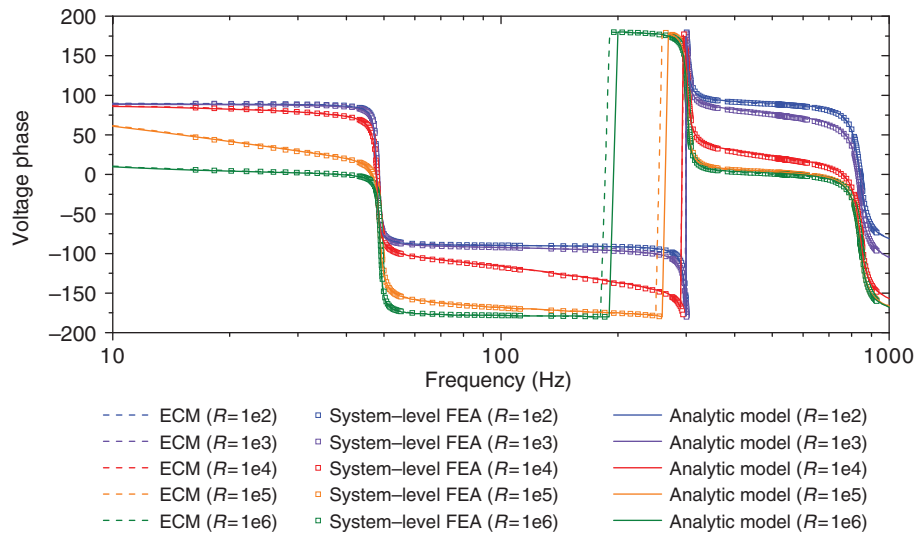
Figure 7. *Phase of output voltage from analytical model, system-level FEA, and equivalent circuit model with various resistive loads.*
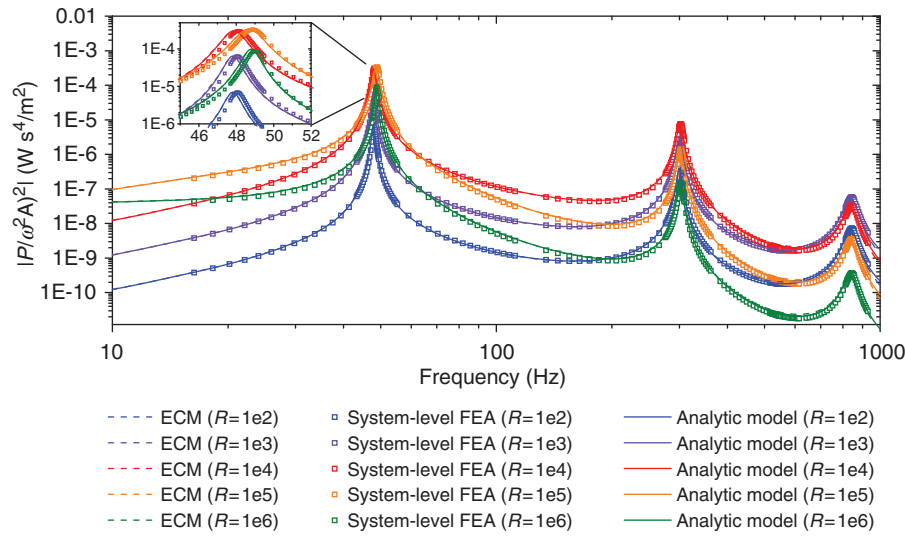
Figure 8. Output power from analytical model, system-level FEA, and equivalent circuit model with various loads.
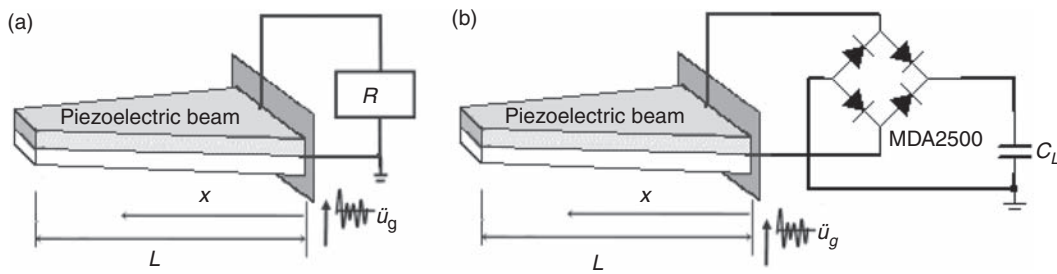
Figure 9. Isosceles trapezoidal unimorph energy harvester subjected to base excitation with (a) a purely resistive load and (b) a practical energy storage circuit attached.

The geometry of energy harvester is more complicated than that in the first validation example. The two parallel sides of the isosceles trapezoid of the beam are of length 15 and 5 mm, respectively. The other geometric and material parameters are the same as those listed in Table 2.

For this example, there is no analytical model available to identify the parameters of the equivalent circuit. Thus, they are identified by the FEA method proposed in the section 'Equivalent Circuit Model with Parameters Identified by FEA'. Again, we consider the first three modes of the system. Figure 10 shows the locus of motional admittance Y_{mot} near resonances obtained from FEA. Applying Equations (15) and (26), we can obtain C_r, L_r, R_r, and N_r from each admittance circle of Y_{mot} in Figure 10. According to Equation (28), we can determine f_r, which is the magnitude of $V_r(t)$, from the charge response at each resonance frequency from FEA. Table 4 lists all the parameters identified from FEA.
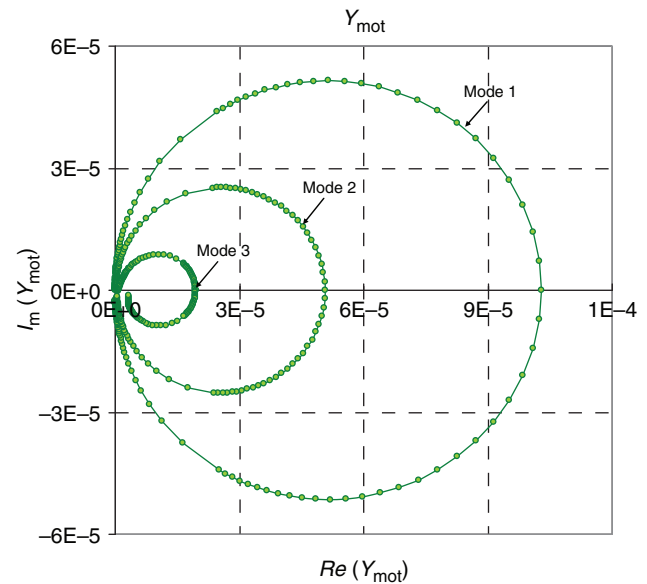
Figure 10. Locus of motional admittance Y_{mot}.

Table 4. Parameters of equivalent circuit model identified from FEA.

r-th mode	C_{dr}	L_{mr}	R_{mr}	C_{mr}	N_r	L_r	R_r	C_r	f_r
1	8.5134E−08	1400.662	9715.873	4.19E−9	0.02672	1	6.9366	5.874E−6	8.30E−2
2	8.4306E−08	340.8209	19722.66	6.67E−10	0.054167	1	57.868	2.274E−7	−5.23E−2
3	8.413E−08	149.5977	51396.43	2.203E−10	0.081759	1	343.56	3.296E−08	3.05E−2
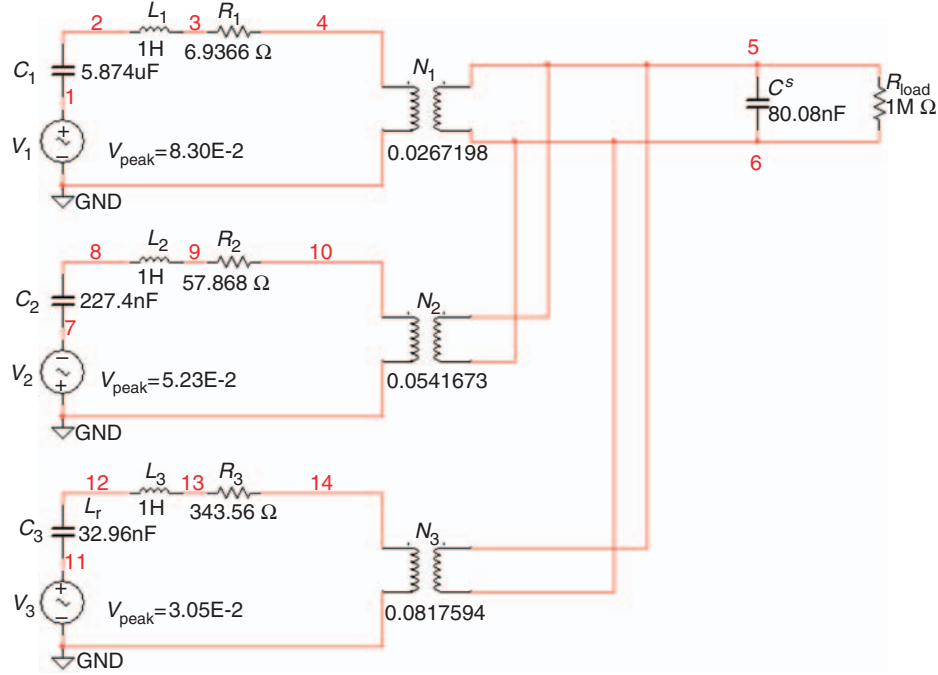
Figure 11. *Multi-mode equivalent circuit model with parameters identified from FEA.*

Finally, we model the equivalent circuit of the energy harvesting system in the SPICE software, as shown in Figure 11. The magnitude of voltage and the power on the electric load by equivalent circuit modeling and system-level FEA are shown in Figures 12 and 13, respectively. Again, excellent agreement in the results of equivalent circuit modeling and system-level FEA is observed, validating the accuracy of the equivalent circuit model with the parameters identified from FEA. Here, FEA is a pre-process to determine the parameters of SPICE simulation. Compared with the coupled FEA–SPICE model given by Elvin and Elvin (2009b), which involves the alternate FEA and SPICE simulation till convergence in each time increment and the computationally expensive pre-process and post-process at each iteration, the proposed approach based on the equivalent circuit model is much simpler and more efficient. It should be emphasized that although the FEA and SPICE simulation are separately conducted, the equivalent circuit model is able to account for the backward coupling effect in the mechanical domain.

Further Example

As validated in the previous section, the proposed ECM-based modeling method is applied to a more general case considering complicated mechanical condition and practical circuit including non-linear electrical elements, which the analytical model and system-level FEA cannot deal with. Here, we consider the same structure of the unimorph energy harvester as that in validation example 2 but replace the purely resistive load with a practical energy storage circuit composed of a rectifier and a energy storage capacitor, as shown in Figure 9(b). Hence the equivalent circuit parameters of the energy harvester are the same as those identified in validation example 2, as listed in Table 4. The full-wave bridge model MDA2500 (manufactured by Motorola) is chosen as the rectifier in the SPICE simulation and six different capacitances of the capacitor C_L are considered for energy storage. The energy accumulated on the storage capacitor can be calculated by $E = C_L V^2 / 2$ and the instant energy harvesting power is approximated by $P = \Delta E / \Delta t$ for a small variation time Δt.

Figures 14 and 15 show the energy accumulation procedure and the instant power on various storage capacitors during one second time, respectively, when the energy harvester is excited at the first natural frequency. It is noted that small capacitors such as 1, 3.3, and 10 µF are quickly charged to saturation, as shown in Figure 14, which means that it is favorable to use up the energy instantly rather than to store it if the attached capacitor is small. While, a large capacitor such as 330 µF is favorable to store the energy for later use because of its larger energy capacity but smaller instant power compared with small capacitors, as shown in Figure 15. However, we will not go further on capacitor selection

and circuit design. The purpose of this example is to illustrate the capability and applicability of the proposed generic ECM-based method. Issues on how to optimize the energy harvesting system with a practical energy storage circuit will be investigated using the proposed ECM-based method in future.

CONCLUSIONS

In summary, various methodologies towards modeling piezoelectric energy harvesters are compared in Table 5. If the maximum achievable power of the system is the concern, the analytical models and
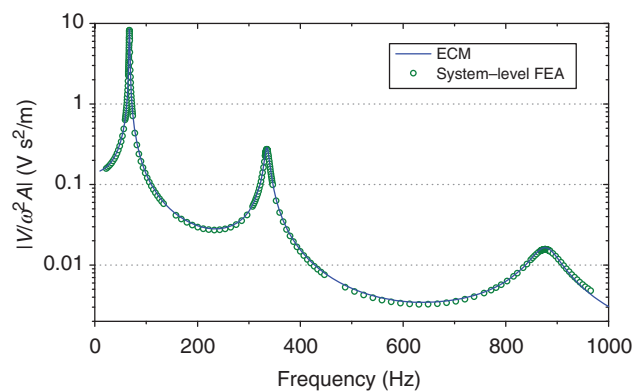

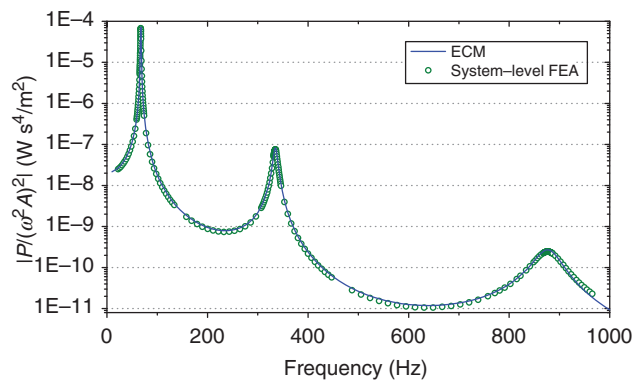**Figure 12.** Magnitude of voltage on the resistor $R = 1\,M\Omega$ by system-level FEA and equivalent circuit model.
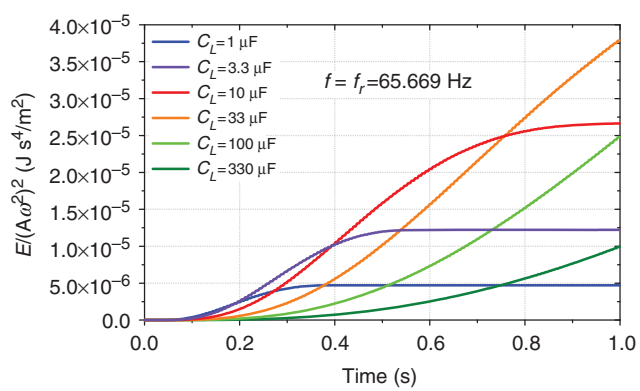

Figure 14. Energy accumulation procedure on the storage capacitor when the harvester is excited at the first natural frequency.
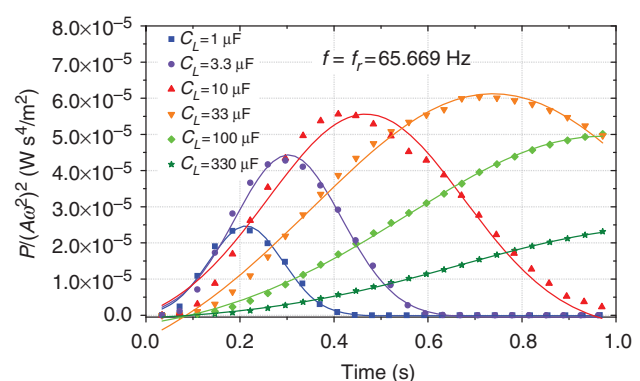

Figure 13. Power on the resistor $R = 1\,M\Omega$ by system-level FEA and equivalent circuit model.

Figure 15. Instant energy harvesting power when the harvester is excited at the first natural frequency.

Table 5. Methodologies for modeling of piezoelectric energy harvesters.

Mechanical condition / Energy harvesting circuit	Simple (e.g., uniform beam with unimorph/bimorph configuration, simple boundaries)	Complex (e.g., non-uniform beam with complex profile or multilayers, complex boundaries)
Only linear elements included (resistor, capacitor, and inductor)	Analytical model	System-level FEA
Non-linear elements (e.g., rectifier, DC–DC converter, and energy storage module) included	Equivalent circuit model (with parameters determined by theoretical modal analysis)	Equivalent circuit model (with parameters identified by FEA)

system-level FEA can be employed for system evaluation. When the practical energy harvesting circuit is considered in system design, the equivalent circuit model-based method proposed in this article is recommended to address the challenges of accurate modeling of the electromechanical coupling system. The parameters used in the equivalent circuit model can be identified by theoretical analysis or FEA according to different mechanical conditions. Two validation examples are investigated and the results demonstrate the accuracy of the proposed equivalent circuit modeling method and its capability of accounting for the backward coupling effect in the piezoelectric energy harvesting system.

Although we consider a single resistor as the energy harvesting circuit in the two validation examples, for the purpose of comparison with the analytical model and system-level FEA, the method developed is applicable for complicated practical circuit including non-linear electric components, as shown in the last example. For piezoelectric energy harvesters with linear structural behavior, the ECM-based method proposed in this article supplies a generic solution for system modeling and evaluation.

REFERENCES

Anton, S.R. and Sodano, H.A. 2007. "A Review of Power Harvesting Using Piezoelectric Materials (2003–2006)," *Smart Materials and Structures*, 16:R1–R21.

Badel, A., Guyomar, D., Lefeuvre, E. and Richard, C. 2005. "Efficiency Enhancement of a Piezoelectric Energy Harvesting Device in Pulsed Operation by Synchronous Charge Inversion," *Journal of Intelligent Material Systems and Structures*, 16:889–901.

Elvin, N.G. and Elvin, A.A. 2009a. "A General Equivalent Circuit Model for Piezoelectric Generators," *Journal of Intelligent Material Systems and Structures*, 20:3–9.

Elvin, N.G. and Elvin, A.A. 2009b. "A Coupled Finite Element-circuit Simulation Model for Analyzing Piezoelectric Energy Generator," *Journal of Intelligent Material Systems and Structures*, 20:587–595.

Erturk, A. and Inman, D.J. 2008a. "A Distributed Parameter Electromechanical Model for Cantilevered Piezoelectric Energy Harvesters," *Journal of Vibration and Acoustics*, 130:041002.

Erturk, A. and Inman, D.J. 2008b. "Issues in Mathematical Modeling of Piezoelectric Energy Harvesters," *Smart Materials and Structures*, 17:065016.

Ikeda, T. 1990. *Fundamentals of Piezoelectricity*, Oxford University Press, Oxford.

Lefeuvre, E., Badel, A., Richard, C. and Guyomar, D. 2005. "Piezoelectric Energy Harvesting Device Optimization by Synchronous Electric Charge Extraction," *Journal of Intelligent Material Systems and Structures*, 16:865–876.

Liao, Y. and Sodano, H.A. 2008. "Model of a Single Mode Energy Harvester and Properties for Optimal Power Generation," *Smart Materials and Structures*, 17:065026.

Liao, Y. and Sodano, H.A. 2009. "Optimal Parameters and Power Characteristics of Piezoelectric Energy Harvesters with an RC Circuit," *Smart Materials and Structures*, 18:045011.

Roundy, S., Leland, E.S., Baker, J., Carleton, E., Reilly, E., Lai, E., Otis, B., Rabaey, J.M., Wright, P.K. and Sundararajan, V. 2005. "Improving Power Output for Vibration-based Energy Scavengers," *IEEE Pervasive Computing*, 4:28–36.

Tilmans, H.A.C. 1996. "Equivalent Circuit Representation of Electromechanical Transducers—Part I: Lumped-parameter Systems," *Journal of Micromechanics and Microengineering*, 6:157–176.

Tilmans, H.A.C. 1997. "Equivalent Circuit Representation of Electromechanical Transducers—Part II: Distributed-parameter Systems," *Journal of Micromechanics and Microengineering*, 7:285–309.